Journal of Applied Fluid Mechanics, Vol. 9, No. 1, pp. 169-176, 2016.
Available online at www.jafmonline.net, ISSN 1735-3572, EISSN 1735-3645.
DOI: 10.18869/acadpub.jafm.68.224.23991

Unsteady/Steady Hydromagnetic Flow of Reactive Viscous Fluid in a Vertical Channel with Thermal Diffusion and Temperature Dependent Properties

I. J. Uwanta† and M. M. Hamza

Department of Mathematics, Usmanu Danfodiyo University, Sokoto, P.M.B. 2346, Nigeria

†*Corresponding Author Email: hmbtamb@yahoo.com*

(Received August 19, 2014; accepted November 10, 2014)

ABSTRACT

The problem of unsteady as well as steady hydromagnetic natural convection and mass transfer flow of viscous reactive, incompressible and electrically conducting fluid between two vertical walls in the presence of uniform magnetic field applied normal to the flow region is studied. Thermal diffusion, temperature dependent variable viscosity and thermal conductivity are assumed to exist within the channel. The governing partial differential equations are solved numerically using implicit finite difference scheme. Results of the computations for velocity, temperature, concentration, skin friction, rate of heat and mass transfer are presented graphically to study the hydrodynamic behavior of fluid in the channel.

Keywords: Thermal diffusion; Variable thermal conductivity; Variable viscosity; Natural convection; Heat transfer; Mass transfer.

1. INTRODUCTION

In many previous studies, the thermal conductivity and viscosity of the saturating fluids was usually assumed to be a constant. This approximation works well as the fluid thermal conductivity and viscosity depend weakly on temperature or the temperature difference is small compared with the average temperature of the system. As the fluid thermal conductivity and viscosity strongly depend on temperature or temperature difference is very large, the thermal conductivity and viscosity are not negligible and will influence the fluid flow and heat transfer behavior significantly. To accurately predict flow behavior and heat transfer rate, it is necessary to take into account the variation of thermal conductivity and viscosity (Elbarbary and Elgazery, 2004). Most of the practical situations demand for physical properties with variable characteristics. Examples of such engineering areas are nuclear plants, gas turbines and various propulsion devices for aircraft, missiles, satellites and space vehicles. Arunachalam and Rajappa (1978) reported forced convection in liquid metal with variable thermal conductivity. Chiam (1996, 1998) investigated the effect of variable thermal conductivity on heat transfer. Abdou (2010) studied effect of radiation with temperature dependent viscosity and thermal conductivity on unsteady flow over a stretching sheet. Khan *et al.* (2011) examined the effect of variable viscosity and thermal conductivity on a thin film flow over a shrinking/stretching sheet. Siddheshwar *et al.* (2014) investigated heat transfer flow in a Newtonian liquid with temperature dependent properties over an exponentially stretching sheet. Uwanta and Hamza (2014b) studied unsteady flow of reactive viscous, heat generating/absorbing fluid with Soret and variable thermal conductivity.

On the other hand, the study of hydromagnetic fluid flow is of considerable important in nuclear engineering control, plasma aerodynamics, mechanical engineering, manufacturing processes, astrophysical fluid dynamics and magnetohydrodynamic (MHD) energy systems (Shercliff, 1965, Sutton and Sherman, 1965, Cramer and Pai, 1973). In view of the applications of MHD, variable viscosity and thermal conductivity, Seddeek *et al.* (2007, 2009) studied hydromagnetic flow in the presence of variable viscosity and thermal conductivity. El-Aziz (2007) investigated temperature dependent viscosity and thermal conductivity effects on MHD three dimensional flows over a stretching surface. MHD generalized Couette flow with variable viscosity and electrical conductivity have been studied by Makinde and Onyejekwe (2011). Seddeek and Salama (2007) presented numerically the effects of variable viscosity and thermal conductivity on unsteady MHD convective heat in a vertical moving plate.

Attia (2008) reported unsteady hydromagnetic Couette flow of dusty fluid with temperature dependent viscosity and thermal conductivity under exponentially decaying pressure gradient. Effects of variable viscosity and thermal conductivity on MHD flow of non-Newtonian fluid over a stretching sheet have been reported by Salem (2007) and Abdel-Rahman (2013). Choudhury and Hazarika (2013) reported effects of variable viscosity and thermal conductivity on MHD oscillatory flow past a vertical plate in slip flow regime with variable suction and periodic plate temperature. Recently Pal and Mondal (2014) examined the effects of temperature dependent viscosity and variable thermal conductivity on MHD non-Darcy mixed convective diffusion of species over a stretching sheet. Ghosh *et al.* (2014) studied temperature dependence of fluid viscosity in hydromagnetic flow. Uwanta and Hamza (2014a) reported unsteady natural convection flow of reactive hydromagnetic fluid in a moving vertical channel.

The purpose of this article is to analyze unsteady as well as steady state hydromagnetic natural convection and mass transfer flow of viscous reactive, incompressible and electrically conducting fluid between two infinite vertical parallel walls in the presence of thermal diffusion, variable viscosity and variable thermal conductivity. In this paper, it is assumed that the conducting fluid is subjected to an exothermic chemical reaction of Arrhenius kinetics. This type of flow found applications in chemical engineering, petroleum industries, and lubrication engineering in improving the productivity and usefulness of the hydromagnetic lubrication used in engineering systems.

2. MATHEMATICAL MODEL

Consider the unsteady flow of an incompressible, electrically conducting, variable viscosity, variable thermal conductivity, viscous reactive fluid between two vertical walls under the influence of a transversely magnetic field of strength B_0 as shown in fig.1. The fluid has small electrical conductivity and electromagnetic force produced is also very small. Initially, it is assumed that both the fluid and the walls are at rest and at same temperature and concentration $T_0^{'}$ and $C_0^{'}$ respectively. At time $t'>0$, the temperature and concentration of the wall $y'=0$ is raised to $T_\omega^{'}$ and $C_\omega^{'}$, and that of $y'=H$ is lowered to $T_0^{'}$ and $C_0^{'}$ respectively such that $T_\omega^{'}>T_0^{'}$ and $C_\omega^{'}>C_0^{'}$ which is thereafter maintained constant. The Soret effect is taken into account. The fluid temperature dependent variable viscosity is of type given by Kafoussias and Willians (1995) $\bar{\mu}=\dfrac{\mu_0}{\left[1+\gamma\left(T'-T_0^{'}\right)\right]}$, where μ_0 is the initial fluid dynamic viscosity at the temperature, $T_0^{'}$, and the variable thermal conductivity is assumed to be of the form (Elbarbary and Elgazery, 2004) $k_f=k_0\left\{1+m^*\left(T'-T_0^{'}\right)\right\}$, where k_0 is the thermal conductivity of the ambient fluid and m^* is a constant depending on the nature of the fluid, where $m^*>0$ for fluids such as water and air, while $m^*<0$ for fluids such as lubrication oils (Elbarbary and Elgazery, 2004). We choose Cartesian coordinate system with the x' axis along the upward direction and the y' axis normal to it. Under these assumptions along with the Boussinesq's approximation, the governing equations can be written as

$$\frac{\partial u'}{\partial t'}=\frac{\partial}{\partial y'}\left(\bar{\mu}\frac{\partial u'}{\partial y'}\right)+g\beta(T'-T_0^{'})+g\beta^*(T'-T_0^{'})-\frac{\sigma B_0^2}{\rho}u' \tag{1}$$

$$\frac{\partial C'}{\partial t'}=D_m\frac{\partial^2 C'}{\partial y'^2}+\frac{D_m k_T}{T_m}\frac{\partial^2 T'}{\partial y'^2} \tag{2}$$

$$\frac{\partial T'}{\partial t'}=\frac{1}{\rho c_p}\frac{\partial}{\partial y'}\left[k_f\frac{\partial T'}{\partial y'}\right]+\frac{QC_0^*A}{\rho C_p}e^{\left(\frac{-E}{RT'}\right)} \tag{3}$$

The initial and boundary conditions for the present problem are

$$\left.\begin{array}{l} t'\le 0: u'=0,\ T'\to T'_0,\ C'\to C'_0,\ 0\le y'\le H \\ t'>0: u'=0, T'=T_\omega^{'},\ C'=C_\omega^{'}\ \ at\ \ y'=0 \\ \qquad u'=0,\ T'=T_0^{'},\ C'=C_0^{'}\ \ as\ \ y'\to H \end{array}\right\} \tag{4}$$

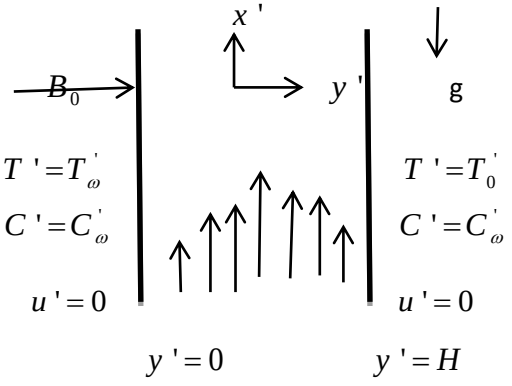

Fig. 1. Schematic diagram of the physical model and coordinate system

where σ is the conductivity of the fluid, B_0 is the electromagnetic induction, β is the coefficient of thermal expansion, β^* is the coefficient of concentration expansion, Q is the heat of reaction, A is the rate constant, E is the activation energy, R is the universal gas constant, ν is the kinematic viscosity, C_0^* is the initial concentration of the reactant species, g is the gravitational force, C_p is the specific heat at constant pressure, k is the thermal conductivity of the fluid, ρ is the density

of the fluid, D_m is the coefficient of mass diffusivity, T_m is the mean fluid temperature, and k_T is the thermal diffusion ratio.

To solve equations (1) to (4), we employ the following dimensionless variables and parameters

$$\left.\begin{aligned}
&y=\frac{y'}{H},\ t=\frac{t'\mu_0}{H^2},\\
&\lambda=\frac{QC_0^*AEH^2}{RT_0^2}e^{\left(\frac{-E}{RT_0}\right)},\\
&\varepsilon=\frac{RT_0}{E},\ \theta_a=\frac{E(T_\omega-T_0)}{RT_0^2},\\
&Gc=\frac{g\beta^*RC_0^2H^2}{E\mu_0^2},Sc=\frac{\nu}{D_m},\\
&Sr=\frac{k_TT_0^2}{T_mC_0^2},C=\frac{E(C'-C_0)}{RC_0^2},\\
&M=\frac{\sigma B_0^2H^2}{\nu\rho},X=\frac{bRT_0^2}{E},\\
&C_a=\frac{E(C_\omega-C_0)}{RC_0^2},\Pr=\frac{\mu_0\rho C_p}{k},\\
&\theta=\frac{E(T'-T_0)}{RT_0^2},Gr=\frac{g\beta RT_0^2H^2}{E\mu_0^2},\\
&\delta=\frac{m^*RT_0^2}{E},U=\frac{u'}{\mu_0},
\end{aligned}\right\} \tag{5}$$

Using (5), the equations (1) to (4) take the following form:

$$\frac{\partial U}{\partial t}=\frac{\partial}{\partial y}\left((1-X\theta)\frac{\partial U}{\partial y}\right)+Gr\theta+GcC-MU \tag{6}$$

$$Sc\frac{\partial C}{\partial t}=\frac{\partial^2C}{\partial y^2}+Sr\frac{\partial^2\theta}{\partial y^2} \tag{7}$$

$$\frac{\partial\theta}{\partial t}=\frac{(1+\delta\theta)}{\Pr}\frac{\partial^2\theta}{\partial y^2}+\frac{\delta}{\Pr}\left(\frac{\partial\theta}{\partial y}\right)^2+\frac{\lambda}{\Pr}e^{\left(\frac{\theta}{1+\varepsilon\theta}\right)} \tag{8}$$

The initial and boundary conditions in dimensionless form are

$$\left.\begin{aligned}
&u=0,\ \theta=0,\ 0\le y\le1,\ t\le0\\
&t>0: u=0,\ \theta=\theta_a, C=C_a,\ at\ y=0\\
&u=0,\ \theta=0,\ C=0,\ as\ y=1
\end{aligned}\right\} \tag{9}$$

where X, δ, M, Gr, Gc, Sc, Sr, Pr, λ, ε, θ_a, and C_a are variable viscosity parameter, variable thermal conductivity parameter, magnetic parameter, thermal Grashof number, mass Grashof number, Schmidt number, Soret number, Prandtl number, Frank-Kamenetskii parameter, activation energy parameter, ambient temperature, and ambient concentration respectively. The other non-dimensional quantities are the skin friction (C_f), the heat transfer rate (Nu), and the rate of mass transfer (Sh) given as

$$C_f=\left.\frac{\partial U}{\partial y}\right|_{y=0,1},\ Nu=-\left.\frac{\partial\theta}{\partial y}\right|_{y=0,1},\ Sh=-\left.\frac{\partial C}{\partial y}\right|_{y=0,1}$$

where C_f is the skin friction, Nu is the Nusselt number and Sh is the Sherwood number.

3. NUMERICAL SOLUTIONS

The governing equations (6) to (8) with the boundary conditions (9) are solved numerically using implicit finite difference scheme given by Makinde and Chinyoka (2011). We used forward difference formulas for all time derivatives and approximate both the second and first derivatives with second order central differences. The semi-implicit finite difference equation corresponding to equations (6) to (8) are as follows

$$\begin{aligned}
&-r_1\mu U_{j-1}^{(N+1)}+(1+2r\mu_1)U_j^{(N+1)}\\
&\quad-r_1\mu U_{j+1}^{(N+1)}=r_2\mu U_{j-1}^{(N)}\\
&\quad+(1-2r_2\mu-M\Delta t)U_j^{(N)}\\
&\quad+r_2\mu U_{j+1}^{(N)}-r_3\left(\theta_{j+1}^N-\theta_{j-1}^N\right)\left(U_{j+1}^N-U_{j-1}^N\right)\\
&\quad+\Delta tGr\theta_j^N+\Delta tGcC_j^N
\end{aligned} \tag{10}$$

$$\begin{aligned}
&-r_1C_{j-1}^{(N+1)}+(Sc+2r_1)C_j^{(N+1)}\\
&\quad-r_1C_{j+1}^{(N+1)}=r_2C_{j-1}^{(N)}+(Sc-2r_2)C_j^{(N)}\\
&\quad+r_2C_{j+1}^{(N)}+r_4\left(\theta_{j-1}^N-2\theta_j^N+\theta_{j+1}^N\right)
\end{aligned} \tag{11}$$

$$\begin{aligned}
&-r_1q\theta_{j-1}^{(N+1)}+(\Pr+2rq_1)\theta_j^{(N+1)}\\
&\quad-r_1q\theta_{j+1}^{(N+1)}=r_2q\theta_{j-1}^{(N)}+(\Pr-2r_2q)\theta_j^{(N)}\\
&\quad+r_2q\theta_{j+1}^{(N)}+\lambda\Delta t\exp\left(\frac{\theta_j^{(N)}}{1+\varepsilon\theta_j^{(N)}}\right)
\end{aligned} \tag{12}$$

Where $r_1=\xi\Delta t/\Delta y^2$, $r_2=(1-\xi)\Delta t/\Delta y^2$, $r_3=X\Delta t/4\Delta y^2$, $r_4=\delta\Delta t/4\Delta y^2$, $r_5=Sr\Delta t/\Delta y^2$ $\mu=1-X\theta$, $q=1+\delta\theta$ and $0\le\xi\le1$. We chose $\xi=1$ the detailed reasons to this particular selection is documented by Makinde and Chinyoka (2011).

4. RESULTS AND DISCUSSION

The numerical results are obtained by solving equations (10) to (12) using the method described in the previous section for various values of physical parameters to describe the physics of the problem. The non-dimensional parameters that govern the flow are the Prandtl number (Pr), which

is inversely proportional to the thermal diffusivity of the working fluid, the Frank-Kamenetskii parameter (λ), the Soret number (Sr), the Magnetic parameter (M), the thermal Grashof number (Gr), the solutal Grashof number (Gc), the non-dimensional time (t), the Schmidt number(Sc), which is inversely proportional to the mass diffusivity of the working fluid, the variable viscosity parameter (X) and the variable thermal conductivity. For the purpose of discussion, some numerical calculations are carried out for dimensionless velocity (U), temperature (θ), concentration (C), skin friction, rate of heat transfer in terms of Nusselt number, and the rate of mass transfer in terms of Sherwood number. Unless otherwise stated, the values: $\lambda = 0.1$, $Gr = 0.1$, M =1, $Gc = 0.1$, Sr = 0.1 ,X = 0.1, $\theta_T = 1$, $C_T = 1$, Pr = 0.71, Sc = 0.62, $t = 0.1$, $\delta = 0.1$ and $\varepsilon = 0.01$ are used for the investigation. Results obtained are displayed graphically for velocity, temperature, concentration, skin friction, Nusselt number and Sherwood number for various flow parameters

The influence of the Frank-Kamenetskii parameter (λ) and non-dimensional time (t) on temperature and velocity profiles is displayed in Fig.2a and 2b respectively. From Fig.2a it is observed that both unsteady and steady-state temperature of the fluid increases with increasing values of λ. This is physically true since an increase in λ lead to significant increases in the reaction and viscous heating source terms and hence considerably increases the fluid temperature. The temperature is strongly coupled to the velocity through the temperature dependent buoyancy terms and hence the recorded temperature increases (with increasing λ) lead to corresponding increases in the magnitude of the fluid velocity as shown in Fig.2b.

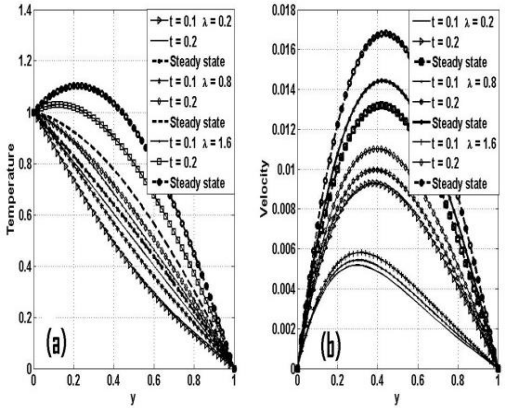

Fig. 2. Variation of unsteady and steady-state temperature and velocity with λ.

The effect of the variable viscosity (X) and magnetic parameter (M) for unsteady as well as steady-state case is shown in Fig.3a and 3b respectively.

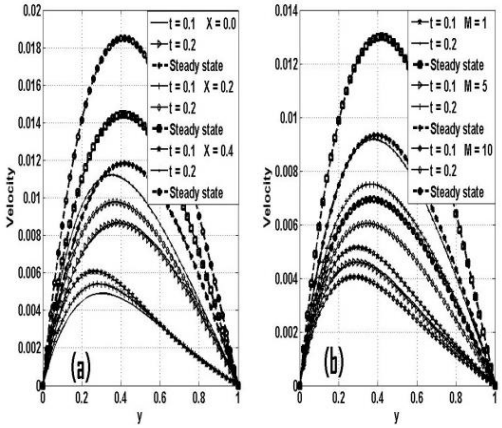

Fig. 3. Variation of unsteady and steady-state velocity with X and M.

In Fig.3a, the graph shows that as X increases, the fluid becomes less viscous and hence their molecular resistance to motion decreases, and thereby increases in fluid flow. It is also seen from Fig.3a that velocity of the fluid is maximum in the vicinity of the hot wall ($y = 0$) and then gradually decreases as it moves towards the cooled wall ($y = 1$). From Fig.3b, as expected, an increasing value of M leads to decreases in both unsteady as well as steady-state fluid velocity. This is due to the increased resistance to flow.

Fig.4a and 4b respectively show the response of the fluid temperature and velocity to variation in the variable thermal conductivity (δ) and time (t). In Fig.4a and 4b it is observed that temperature and velocity of the fluid increases with increasing δ and t until a steady-state condition is attained. This is physically true, since the relation $\delta = m^*\left(T' - T_0'\right)$ indicate that mounting values of δ increase the temperature difference between outside the plate and outside the boundary layer. As a result heat is transferred rapidly from plate to fluid within the boundary layer, that is why both temperature and velocity profiles enlarge due to growing δ. It means that the velocity and thermal boundary layer thickness rise for larger δ.

The effect of the Soret number (Sr) on velocity and concentration profiles is analyzed in Fig.5a and 5b respectively. The Soret effect (Sr) represents the mass energy flux in the flow. It is clear from Fig.5a and 5b that an increase in Sr causes a rise in the velocity and concentration of the fluid. Fig.6a and 6b represent the concentration and velocity distribution for different values of the Schmidt number (Sc) and time (t). The values of Schmidt number (Sc) are chosen for hydrogen (Sc = 0.22), water vapor (Sc = 0.62) at temperature 25^0C and propylbenze (Sc = 2.62). In both Fig.6a and 6b, it is seen that unsteady and steady-state concentration and velocity of hydrogen increase the flow while concentration and velocity of water vapor reduces the flow.

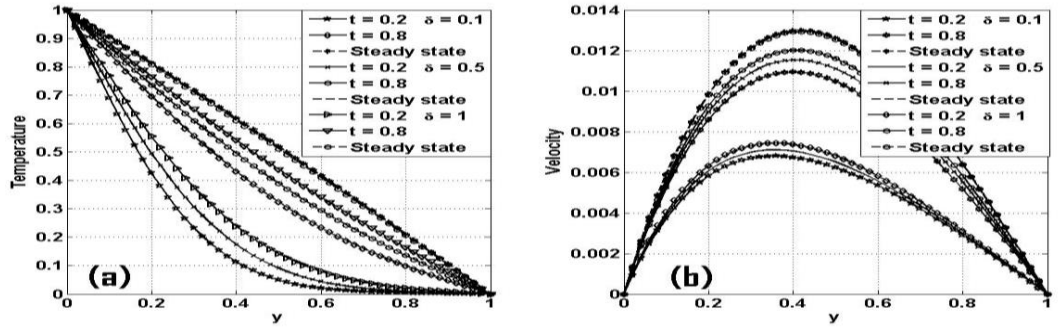

Fig. 4. Variation of unsteady and steady-state temperature and velocity with δ .

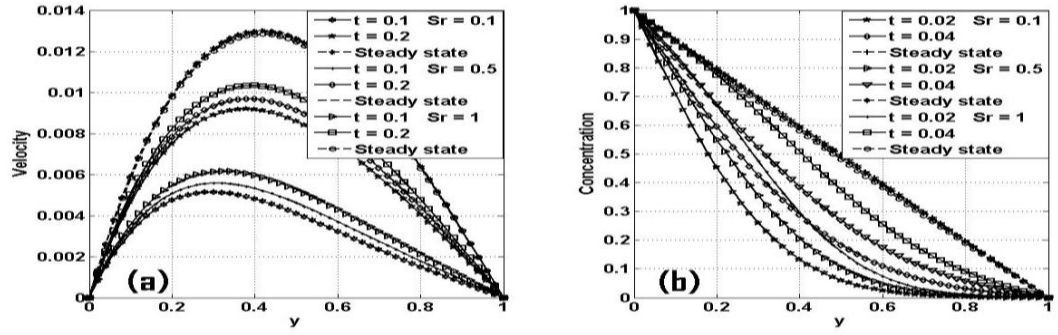

Fig. 5. Variation of unsteady and steady-state velocity and concentration with Sr.

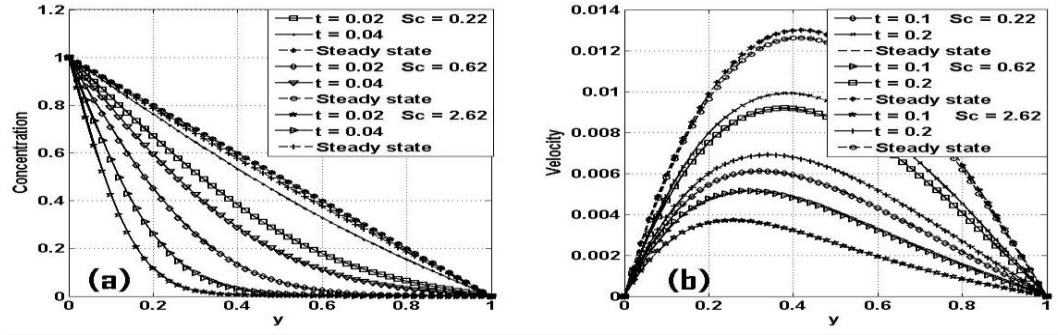

Fig. 6. Variation of unsteady and steady-state concentration and velocity with Sc.

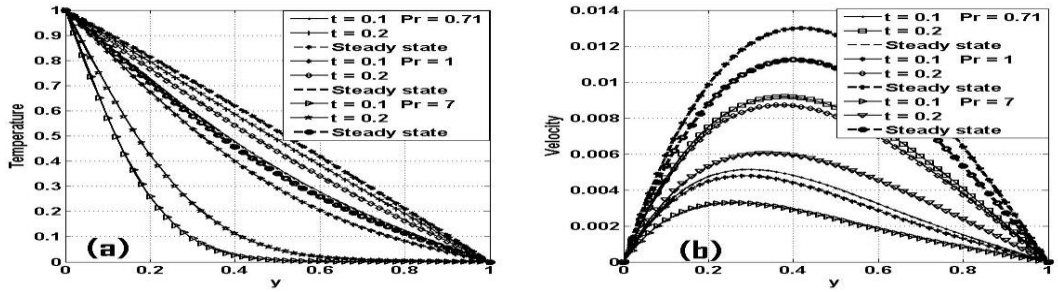

Fig. 7. Variation of unsteady and steady-state temperature and velocity with Pr.

The effect of the Prandtl number (Pr) on the temperature and velocity field is illustrated in Fig.7a and 7b respectively. The values of Pr are chosen for air (Pr = 0.71), electrolyte solution (Pr = 1) and water (Pr = 7). It is noticed from Fig.7a and 7b that temperature and velocity of air increase the fluid flow while temperature and velocity of water decreases both unsteady as well as steady-state fluid flow. Fig.8a and 8b represent the velocity profiles for different values of thermal Grashof number (Gr) and mass Grashof number (Gc) respectively. These plots Fig.8a and 8b indicate that the momentum boundary layer thickness increases with increasing values of Gr and Gc. The consequence of the increased buoyancy source terms due to higher values of Gr and Gc increases both unsteady and steady-state velocity of the fluid.

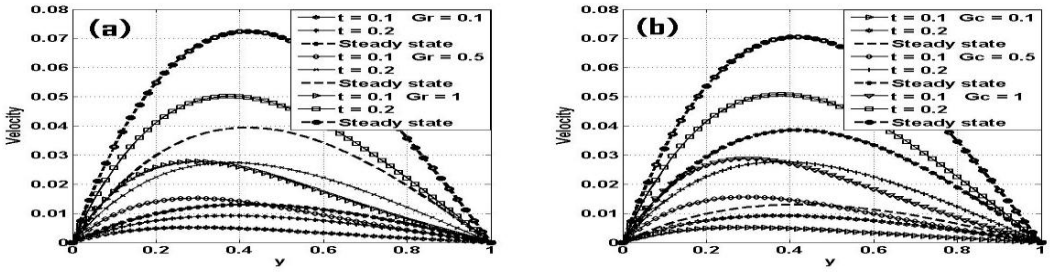

Fig. 8. Variation of unsteady and steady-state velocity with Gr and Gc.

The rate of heat transfer (Nusselt number) and skin friction dependence of Frank-Kamenetskii parameter (λ) for varying values of time (t) at the plate $y = 1$ is illustrated in fig.9a and 9b respectively.

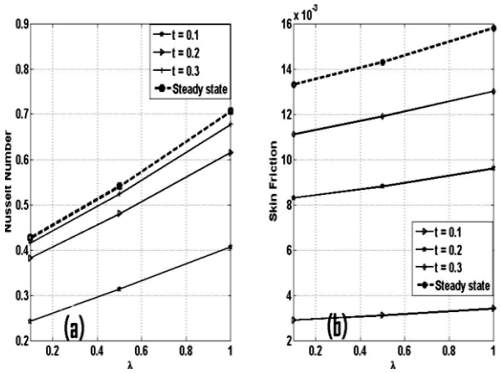

Fig. 9. Variation of unsteady and steady-state Nusselt number and skin friction at $y = 1$ with λ.

From fig.9a and 9b it can be noticed that Nusselt number and skin friction increases with increasing both λ and t until a steady-state condition is achieved. The wall shear stress dependence on variable viscosity (X) and magnetic parameter (M) for varying values of time (t) at the plate $y = 0$ is displayed in fig.10a and 10b respectively. Fig.10a reflected that skin friction increases as X and t increases until a steady-state condition is attained. From fig.10b it is seen that as t increases, the frictional force due to the motion of the fluid also increases until a steady-state condition is reached**.** It is evident from fig.10b that higher values of M reduce the skin friction.

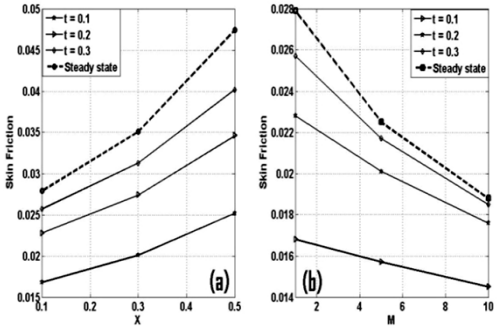

Fig. 10. Variation of unsteady and steady-state skin friction at $y = 0$ with X and M.

Fig.11a and 11b respectively represent the Nusselt number and skin friction dependence on variable thermal conductivity (δ) for varying values of t at the plate $y = 1$.

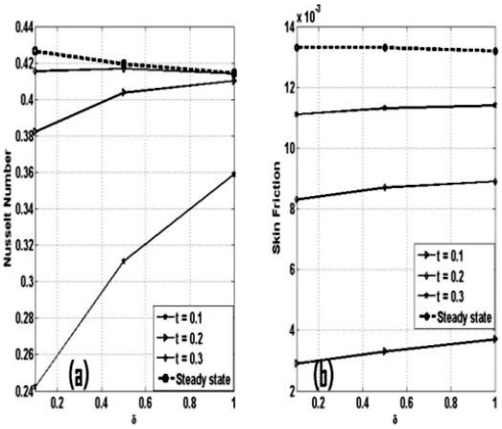

Fig. 11. Variation of unsteady and steady-state Nusselt number and skin friction at $y = 1$ with δ.

These plots indicate that as δ and t increases, Nusselt number and skin friction also increase until a steady-state value is achieved. The rate of mass transfer (Sherwood number) at the plate $y = 1$ is depicted in fig.12a and 12b respectively for varying values of Soret number (Sr). It is clearly seen from these figures that Sherwood number and skin friction increases as Sr and t increase.

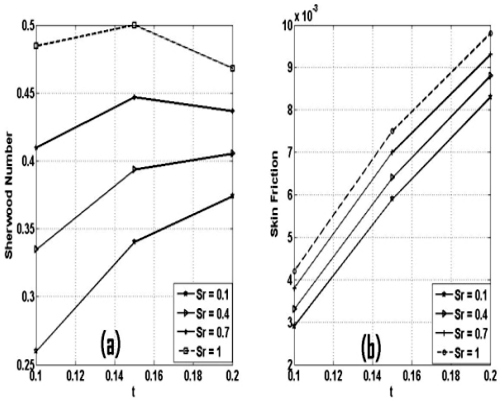

Fig. 12. Variation of unsteady and steady-state Sherwood number and skin friction at $y = 1$ with Gr and Gc.

Fig.13a and 13b show the wall shear stress dependence on Gr and Gc for varying values of t at the plate $y = 0$ respectively. From these figures it is noticed that as t increase, the skin friction also increases until a steady-state value is achieved. Fig.13a and 13b reflected that values of Gr and Gc increase the skin friction.

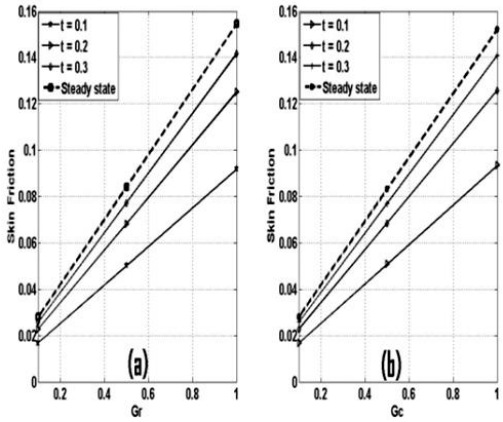

Fig. 13. Variation of unsteady and steady-state skin friction at $y = 0$ with Gr and Gc.

5. CONCLUSION

This paper investigates unsteady as well as steady-state flow of viscous reactive, incompressible and electrically conducting fluid between two infinite vertical parallel walls in the presence of transverse magnetic field, thermal diffusion, variable viscosity, and variable thermal conductivity. The governing equations are solved numerically using implicit finite difference scheme. The main findings can be summarized as follows

(i) Increasing the variable viscosity, chemical reaction, variable thermal conductivity, thermal diffusion, Grashof number and modified Grashof number accelerate the velocity of the fluid, while higher values of magnetic parameter, Schmidt number and Prandtl number reduce the velocity of the fluid.

(ii) Temperature of the fluid increases with increasing values of the reaction strength and variable thermal conductivity, while larger values of Prandtl number reduces the temperature of the fluid.

(iii) Concentration of the fluid increases with increasing values of thermal diffusion parameter and decreases with increasing values of the Schmidt number.

(iv) Frictional force due to the motion of the fluid increases with increasing material parameters (Sr, X, λ, δ, Gr and Gc), while decreases with increasing values of M.

(v) The rate of heat transfer at the channel walls increases with increasing λ and δ

This type of flow can be investigated in different geometries, like cylindrical coordinates, Couette flow etc. and effects of Navies slip on the flow system

ACKNOWLEDGEMENT

The author M.M. Hamza is thankful to Usmanu Danfodiyo University, Sokoto, Nigeria for financial assistance.

REFERENCES

Abdel-Rahman, G. M. (2013). Effects of variable viscosity and thermal conductivity on unsteady MHD flow of non-Newtonian fluid over a stretching porous sheet, *Thermal Sci.* 17, 1035-1047.

Abdou, M. M. M (2010). Effect of radiation with temperature dependent viscosity and thermal conductivity on unsteady a stretching sheet through porous media. *Nonlinear Analysis Modelling and Control* 15, 257-270.

Arunachalam, M. and Rajappa N. R. (1978). Forced convection in a liquid metals with variable thermal conductivity and capacity, *ACTA Mechanica* 31, 25-31

Attia, H. A. (2008). Unsteady hydromagnetic Couette flow of dusty fluid with temperature dependent viscosity and thermal conductivity under exponential decaying pressure gradient, *Commun. Nonlinear Sci. Numer. Simul.* 13, 1077-1088.

Chiam, T. C. (1996). Heat transfer with variable thermal conductivity in a stagnation point flow towards a stretching sheet. *International Communications in Heat and Mass Transfer* 23, 239-248.

Chiam, T. C. (1998). Heat transfer in a fluid with variable thermal conductivity over a linearly stretching sheet. *ACTA Mechanica* 129, 63-72.

Choudhury, M and Hazarika, G. C (2013). The effects of variable viscosity and thermal conductivity on MHD oscillatory free convective flow past a vertical plate in slip flow regime with variable suction and periodic plate temperature. *Journal of Applied Fluid Mechanics* 6(2), 277-283.

Cramer, K. R. and S. I. Pai (1973). *Magnetofluid Dynamics for Engineers and Applied Physicists*, McGraw Hill Book Company, New York

Elbarbary, E. M. E. and Elgazery, N. S. (2004). Chebyshev finite difference method for the effects of variable viscosity and variable thermal conductivity on heat transfer from moving surfaces with radiation. *International Journal of Thermal Science* 43, 889-899.

El-Aziz, M. A. (2007). Temperature dependent viscosity and thermal conductivity effects on combined heat and mass transfer in MHD three

dimensional flow over a stretching surface with ohmic heating. *Meccanica* 42, 375-386.

Kafoussias, N. G. and E. W. Willians (1995). Thermal diffusion and diffusion-thermo effects on mixed free-forced convective and mass transfer boundary layer flow with temperature dependent viscosity. *Int. J. Engng. Sci.* 33, 1369-1384.

Ghosh, SK, G. C Shit and J. C. Misra (2014). Heat transfer in hydromagnetic fluid flows: Study of temperature dependence of fluid viscosity. *Journal of Applied Fluid Mechanics* 7(4) 633-640.

Khan, Y., Q. Wu, N. Faraz and A. Yildirim (2011). The effects of variable viscosity and thermal conductivity on a thin film flow over a shrinking/stretching sheet. *Comp. Math. Appl*. 61 3391-3399.

Makinde, O. D. and O. O. Onyejekwe (2011). A numerical study of MHD generalized Couette flow and heat transfer with variable viscosity and electrical conductivity. *J. Magnetism and Magnetic Materials* 323, 2757-2763.

Makinde, O. D. and T. Chinyoka (2011). Numerical study of unsteady hydromagnetic generalized Couette flow of a reactive third-grade fluid with asymmetric convective cooling. *Computers and Math. Appl*. 61, 1167-1179.

Pal, D. and H. Mondal (2014). Effects of temperature dependent viscosity and variable thermal conductivity on MHD non-Darcy mixed convective diffusion of species over a stretching sheet. *J. Egy. Math. Society* 22 (2014) 123-133.

Salem, A. M. (2007). Variable viscosity and thermal conductivity effects on MHD flow and heat transfer in viscoelastic fluid over a stretching sheet. *Physics Letters A* 369 (2007) 315-322.

Seddeek, M. A and F. A Salama (2007). The effect of temperature dependent viscosity and thermal conductivity on unsteady MHD convective heat transfer past a semi-infinite vertical porous moving plate with variable suction. *Comp. Materials Sci*. 40, 186-192.

Seddeek, M. A, A. A. Darwish and M. S. Abdelmeguid (2007). Effects of chemical reaction and variable viscosity on hydromagnetic mixed convection heat and mass transfer for Hiemenz flow through porous media radiation. *Commun. Nonlinear Sci. Numer. Simulat.* 12, 195-213.

Seddeek, M. A., A. A. Afify and A. M. Al-Hanaya (2009). Similarity solutions for a steady MHD Falkner-Skan flow and heat transfer over a wedge considering the effects of variable viscosity and thermal conductivity. *Appl. Appl. Math*. 4, 301-313.

Shercliff, J. A. (1965). *A Textbook of Magnetohydrodynamic*. Pergoman Press, London.

Siddheshwar, P. G, G. N. Sekhar and A. S. Chethan (2014). Flow and heat transfer in a Newtonian liquid with temperature dependent properties over an exponential stretching sheet. *Journal of Applied Fluid Mechanics* 7(2) 367-374.

Sutton, G.W. and A. Sherman (1965). *Engineering Magnetohydrodynamic*. McGraw Hill Book Company, New York

Uwanta, I. J. and M. M. Hamza (2014a). Unsteady natural convection flow of reactive hydromagnetic fluid in a moving vertical channel. *International Journal of Energy and Technology* 6(9) 1-7.

Uwanta, I. J. and M. M. Hamza (2014b). Unsteady flow of reactive viscous, heat generating/absorbing fluid with Soret and variable thermal conductivity. *International Journal of Chemical Engineering, Article* 1-15.